

Volume Preserving Haptic Pottery

Subhajit Chaudhury*

Subhasis Chaudhuri†

Vision and Image Processing Laboratory, Department of Electrical Engineering
Indian Institute of Technology Bombay, Mumbai-400076

ABSTRACT

This paper proposes a realistic deformation model for pottery in which the user can interact with a rotating clay volume using a haptic tool. The deformation algorithm preserves the volume of clay to model the incompressible nature of semi-solid clay used in pottery. The interactive clay volume consists of an array of cylindrical elements stacked up vertically, providing simple and efficient collision detection and response. As a part of collision response, the force feedback consisting of both normal spring deformation force and friction force is rendered. Volume preservation is achieved by distributing the removed clay due to interactions, to the entire clay volume using a Rayleigh density function. To depict the real life pottery experience, the mechanical stability of the rotating clay volume is also included.

Index Terms: Haptic Rendering, Virtual Pottery, Cylindrical element based rendering, Volume preserving deformation

1 INTRODUCTION

Pottery making is a work of art that has its roots long back in history. Pottery finds its place in almost all cultures of the world in some form or the other. Conventional pottery consists of a semi-solid bulk of clay placed on a rotating platform which is shaped by human hands or certain tools. During the process of pottery, force is experienced by the hands on contact with the rotating clay producing the feeling of touch. In this work we try to reproduce the experience of real life pottery using a haptic device for force feedback. The motivation behind this work is to develop a technique for volume preserving deformation modeling with virtual pottery being an application of the same.

An introduction to haptic rendering techniques is given by Salisbury *et al.*[5][10]. Avila *et al.*[1] used physical properties like stiffness, color and density during voxel representation. Ziles and Salisbury[13] introduced the concept of “god object” based rendering while Ruspini *et al.*[9] introduced proxy based rendering. There are rendering methods which use hybrid approaches[4]. Other methods include proxy based force computation for dense 3D point cloud data by estimating the surface normal at the point of contact[11].

For haptic rendering of deformable objects, the mass-spring-damper model[12] is very popular for its simplicity and computational efficiency. In such systems objects are synthesized by mesh structures and model deformation is computed by solving the dynamics of the mass-spring-damper system for mass points located on the vertices of the mesh. Even if such systems model elastic deformation quite well, they cannot be used for modeling clay deformation. A plastic deformation model is given by [7] which models Gaussian deformation of the vertices around the point of contact, but it is not a very realistic volume deformation model.

*e-mail: subhajitiitb@ee.iitb.ac.in

†e-mail:sc@ee.iitb.ac.in

Virtual Pottery is a special case of rendering deformable objects. In the recent past, attempts have been made to model clay deformations. The dynamic subdivision solids based modeling[8] implemented the haptic sculpting of virtual clay. An iso-surface based representation of clay is given by [2]. The long elements method[3] models physics based elastic deformation in longitudinal direction. The circular sector element method[6] models virtual pottery by considering that the clay volume is consisted of circular sectors and interaction with each such sector produces deformation. However the previous works do not focus on preserving the mass of the rotating clay body. Furthermore in most of the previous works the haptic tool interacting with the clay model is assumed to be spherical. In this work, we proposed a volume preserving algorithm for rendering haptic pottery using a generic haptic interacting tool structure. We considered clay density constant at all parts of the clay body and density is assumed not to change with time. Hence the mass conservation constraint is effectively converted to a constraint on preserving the volume. We also investigated the mechanical stability issues of the model for producing a better depiction of real life pottery, which was missing in the previous works.

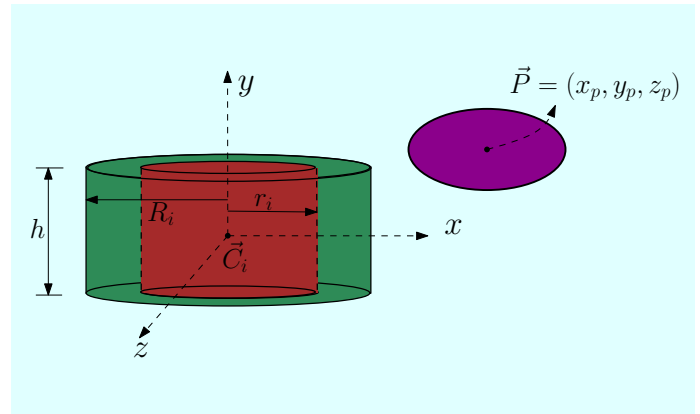


Figure 1: An enlarged view of a cylindrical element and an elliptical haptic tool, \vec{P} .

The organization of the paper is as follows. Section 2 explains the assembly of the cylindrical elements to form the rotating clay body, along with the notations used in the paper. Section 3 gives the structure of the generic haptic interactive tool. The collision detection algorithm is discussed in section 4. The volume preserving deformation model is illustrated in section 5. Force feedback algorithm is discussed in section 6. Section 7 gives the mechanical stability aspects of the model. In section 8 we illustrate the efficiency and outcome of our algorithm for certain test cases and offer conclusion to the paper.

2 BULK CLAY MODEL

During real-life pottery, we encounter a bulk of semi-solid clay rotating on a platform. Since the clay body is radially symmetric about its axis of rotation, an array of cylinders, each with

fixed height, would best approximate the rotating virtual clay body. These cylinders are stacked up vertically to form the consolidated bulk clay model.

The clay body is initially assumed to be composed of N cylinders, where N can change during execution of the algorithm (this is discussed in section 5.1). For the i^{th} cylinder, the centroid is given by $\vec{C}_i = \{x_i, y_i, z_i\}$. As shown in figure 1, the assumed co-ordinate system has y -axis as the vertical direction. Thus in order to stack up cylinders their y -values must increase by the height of the cylinder. Therefore we have, $\forall i \in 1$ to N , $x_i = x_{i-1}, y_i = y_{i-1} + h, z_i = z_{i-1}$, where the bottom most element is located at origin, $x_1 = 0, y_1 = 0, z_1 = 0$. Each cylinder is attributed with an external radius of R_i and internal radius of r_i .

The haptic interface point(HIP) is the manifestation of the physical haptic device in the virtual space. The HIP is represented by $\vec{P} = (x_p, y_p, z_p)$ as shown in figure 1.

3 STRUCTURE OF THE HAPTIC TOOL

The object that interacts with the rotating clay model gives it the appropriate shape. In actual pottery, the potter's hand can assume different shapes while interacting with the clay to give it necessary shape. The shape that is chosen, affects the nature of clay deformation and also the resultant force feedback. So defining a generic structure of the haptic tool is a useful addition to make virtual pottery more realistic.

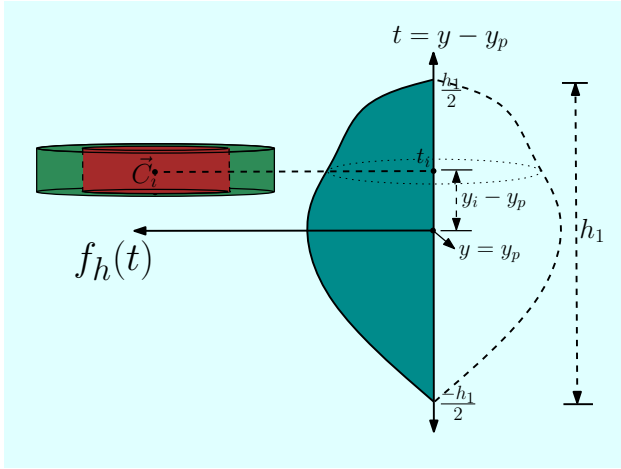


Figure 2: Illustration of a generic haptic interaction tool profile which is radially symmetric in the x - z plane.

To model the generalized structure of the haptic interacting tool, we first assume that the tool is radially symmetric about the unit vector directed along the y -axis. If the cross section of the tool is taken in the x - y plane, then it's radial length with its center being the HIP at a given height is given by $f_h(y - y_p)$, where $f_h(\cdot)$ is assumed to be a continuous function of y . For the ease of representation, we assume $t = y - y_p$. Thus the t -axis shown in figure 2 is the y -axis shifted by y_p to center the haptic tool at the HIP. The tool cross section shown in figure 2 is a generic function whereas the tool shown in figure 1 is elliptical which is given as, $f_h(t) = b\sqrt{1 - \frac{t^2}{a^2}}$ where constants a and b vary the eccentricity of the ellipse.

The extent of the haptic tool in the y -direction is shown as h_1 in figure 2. Without any loss of generality, it is assumed that the length h_1 is equally distributed on either side of $t = 0$ point.

4 COLLISION DETECTION

When the haptic tool and the rotating clay occupy the same space at the same time, then collision is said to occur. Collisions in the virtual world represent the interaction of the human hand with the rotating bulk clay in actual pottery.

For the purpose of collision detection, we divide the problem into a two stage problem. Firstly we find out which cylinders are the potential candidates that can collide with the haptic tool for the current HIP. We store the indices of those cylindrical elements in a selection list L . Next, out of these potential candidates, we find out which cylindrical elements actually collide with the haptic tool. Breaking the problem into two stages reduces the computation time which otherwise would have been computationally expensive if linear search was employed.

To find which cylindrical elements can potentially collide with the tool, we find out the span of the haptic tool in the y -direction for the current HIP. If y_p is the current y -value of the HIP, then the tool spans from $y_p - \frac{h_1}{2}$ to $y_p + \frac{h_1}{2}$ in the y -direction. Using these bounds, we find the indices of the elements closest to either of the extremes of the tool. If top represents the upper index and $bottom$ the lower index, we have

$$top = \min(N, \lceil \frac{y_p + \frac{h_1}{2}}{h} \rceil) \quad (1)$$

$$bottom = \max(1, \lfloor \frac{y_p - \frac{h_1}{2}}{h} \rfloor), \quad (2)$$

where h_1 is the y -extent of the tool and h is the height of each cylinder. The value of top cannot exceed the number of cylinders and $bottom$ cannot be less than 1.

The selection list L comprises of all indices from $bottom$ to top , $L = \{bottom, bottom + 1, \dots, top - 1, top\}$, which are potential candidates for collision.

Having found the list of potential candidates for collision, we have to find out which cylinders do actually collide with the tool. For this purpose we define an indicator vector, \vec{S} . The i^{th} entry of \vec{S} is 1 if the i^{th} cylinder collides with the tool, otherwise 0.

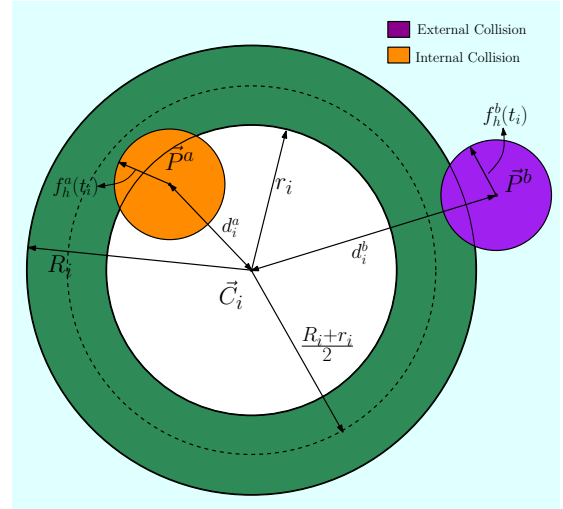


Figure 3: Collision of the haptic tool with the i^{th} cylindrical element showing the dashed demarcating circle. The values for expansive collision are super-scripted by a and that for compressive collision by b .

Now to investigate if the i^{th} cylinder has collided with the tool, the first condition it has to satisfy is that i should be in the selection list L . If i is in the selection list, we calculate the distance from its centroid \vec{C}_i to the HIP, given by

$$d_i = \sqrt{(x_p - x_i)^2 + (z_p - z_i)^2}$$

Having calculated d_i , we classify the collision of the haptic tool with the clay body into two types. When the haptic tool collides with the external surface of the clay body, we term it as compression of clay or compressive collision and when the tool collides with the internal surface we term it expansive collision.

To demarcate between compressive and expansive collision, for each cylinder we specify a fictitious circle called the demarcating circle, whose radius, r_{d_i} is given by $r_{d_i} = \frac{R_i + r_i}{2}$. If the distance d_i is greater than r_{d_i} , we classify the collision as compressive type otherwise it is of expansive type

An external collision occurs, as shown in figure 3, when distance between centroid and HIP is less than sum of external radius and tool radial length, $d_i < (R_i + f_h(t_i))$.

Thus the indicator vector S in this case is given by

$$S = \{s_i | s_i \in \{0, 1\}, \quad s_i = I(i \in L \text{ and } d_i < R_i + f_h(t_i))\}$$

where $I(\text{condition})$ is 1 if the *condition* is true, otherwise 0. Similarly collision from inside occurs if the sum of d_i and $f_h(t_i)$ exceeds the internal radius of the cylinder. The vector S in this case is,

$$S = \{s_i | s_i \in \{0, 1\}, \quad s_i = I(i \in L \text{ and } d_i + f_h(t_i) > r_i)\}$$

For a general shape of the haptic interaction tool, it may be possible that for some values of i , $d_i < R_i + f_h(t_i)$ while for others $d_i + f_h(t_i) > r_i$. However, the interaction can be either expansive or compressive. Hence we check the collision conditions at $t = 0$ (center of the tool) to decide the nature of collision.

5 DEFORMATION

For compressive collision, the external radii of the cylindrical elements are decreased to render compression of clay. Similarly for the expansive collision case, the internal radii are increased. The decrease in these radii is by the amount ϵ_{r_i} , where ϵ_{r_i} is proportional to $(R_i - r_i)$.

For compression, the external radius is decreased by ϵ_{r_i} as collision response.

$$R_i^{new} = R_i - \epsilon_{r_i} \cdot s_i. \quad (3)$$

Similarly for the expansion, the internal radius of the i^{th} cylinder is increased by ϵ_{r_i}

$$r_i^{new} = r_i + \epsilon_{r_i} \cdot s_i. \quad (4)$$

where s_i is the collision indicator variable and i ranges from 1 to N .

The reason for choosing ϵ_{r_i} as an increasing function of $(R_i - r_i)$, is to ensure the reduction of ϵ_{r_i} as the cylinder becomes thinner. This is necessary to minimize the chances of holes being formed which occurs when external radius R_i becomes less than r_i . Also the choice of such ϵ_{r_i} ensures better mechanical stability of the system. This is discussed in detail in section 7.

5.1 Volume Preservation

The reduction in volume as conveyed by equations (3) and (4) is not volume preserving. It just produces the effect of removing the clay volume from the point of contact. But in real pottery since soft and wet semi-solid clay has deformation property that is volume preserving (assuming constant density), our clay modeling algorithm should also preserve volume.

In real pottery, the clay removed from the point of contact is redistributed to the other parts of the clay body, which is exactly the principle for our volume preserving algorithm. Let $\Delta v'$ be the volume of removed clay due to collision with the haptic tool.

For compressive collision, the volume of removed clay $\Delta v'$ is change in volume due to reduction in external radius, given by

$$\Delta v' = \pi \sum_{i=1}^N s_i \{R_i^2 - (R_i - \epsilon_{r_i})^2\} \cdot h = \pi \sum_{i=1}^N s_i \epsilon_{r_i} (2R_i - \epsilon_{r_i}) \cdot h$$

Similarly, for expansive collision, the removed clay volume is given by,

$$\Delta v' = \pi \sum_{i=1}^N s_i \epsilon_{r_i} (2r_i + \epsilon_{r_i}) \cdot h$$

Denoting normalized removed volume as $\Delta v = \frac{\Delta v'}{\pi h}$

$$\Delta v = \begin{cases} \sum_{i=1}^N s_i \epsilon_{r_i} (2R_i - \epsilon_{r_i}), & \text{for compression} \\ \sum_{i=1}^N s_i \epsilon_{r_i} (2r_i + \epsilon_{r_i}), & \text{for expansion} \end{cases}$$

The normalized removed volume is redistributed both to the internal and external clay surface as shown in figure 4. Thus the normalized removed volume is split into two components, Δv_{int} representing the volume redistributed to the internal surface and similarly Δv_{ext} for external surface volume redistribution.

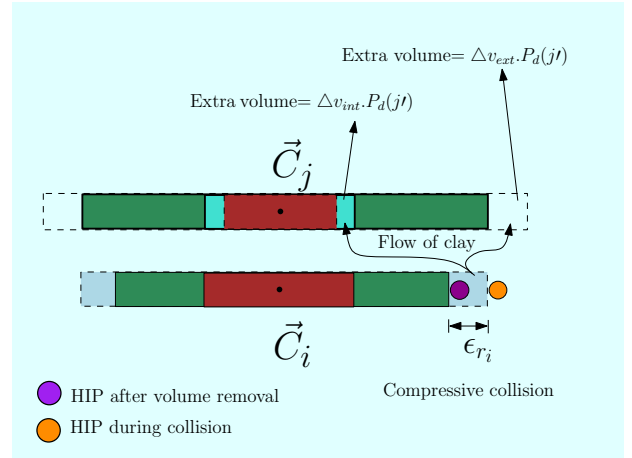


Figure 4: Illustration of flow of clay due to compressive collision from an element to an element placed above it. The removed clay is distributed into two parts for the internal and the external surfaces. It is assumed that $j > top$ and $j' = j - top$

We define α , the volume redistribution ratio, which denotes the amount of removed volume that is added to the internal surface. Thus,

$$\Delta v_{int} = \alpha \Delta v \quad \text{and} \quad \Delta v_{ext} = (1 - \alpha) \Delta v$$

where α has value between 0 and 1. For compressive and expansive collision, α is empirically assigned a value between 0.25 and 0.3, implying internal volume expansion is lesser than its external counterpart. The addition of clay volume on the internal surface is carried out keeping in mind that the internal free volume must be greater than Δv_{int} , otherwise it would violate volume preservation norms. So if $r_i = 0, \forall i$ there is no Δv_{int} .

The removed clay volume is distributed in the local neighborhood along the y-axis following the Rayleigh distribution function, given by

$$Q_p(x) = \begin{cases} \frac{x}{\sigma^2} e^{-x^2/2\sigma^2} & , x \geq 0 \\ 0 & , x < 0 \end{cases}$$

where the spread of the clay volume is governed by the variance $\frac{\sigma^2}{2}(4 - \pi)$. The Rayleigh function attains a peak at a non-zero value, thus modeling clay movement at a certain distance from the point of collision. Since the cylinders defining the clay are of constant height h , the discrete distribution function is obtained as

$$P_d(j) = \frac{Q_p(hj)}{\sum_{k=1}^{L_1} Q_p(hk)}, \quad \text{for } j = 1, 2, \dots, L_1$$

where $P_d(j)\Delta v$ is the additional volume to be added to the j^{th} cylinder, up to L_1 number of such cylinders. Since $\sum_{j=1}^{L_1} P_d(j) = 1$, the total volume is preserved. But along which direction should we add this volume?

The redistribution of clay is decided by the momentum of the haptic interacting tool. If the haptic tool has positive vertical velocity then clay is redistributed in the positive y direction. Clay addition to the cylindrical elements effectively results in increase of external radius and decrease of internal radius. For flow of clay in the upper cylindrical elements starts from the $(top + 1)^{\text{th}}$ element. Equations (5) and (6) gives the change in radius for this scenario

$$R_j^{\text{new}} = \sqrt{R_j^2 + P_d(j - top) \cdot \Delta v_{\text{ext}}} \quad (5)$$

$$r_j^{\text{new}} = \sqrt{r_j^2 - P_d(j - top) \cdot \Delta v_{\text{int}}} \quad (6)$$

where, $top < j \leq \min(top + L_1, N)$. The event in which $top + L_1$ exceeds N the clay would be distributed in a region where no cylinders are defined. So index i is upper bounded by $\min(top + L_1, N)$.

Similarly for haptic tool movement in the negative vertical direction, clay flow would be to the lower cylindrical elements starting from element indexed by $bottom - 1$. Thus the radius update equations are

$$R_j^{\text{new}} = \sqrt{R_j^2 + P_d(bottom - j) \cdot \Delta v_{\text{ext}}} \quad (7)$$

$$r_j^{\text{new}} = \sqrt{r_j^2 - P_d(bottom - j) \cdot \Delta v_{\text{int}}} \quad (8)$$

where $\max(1, bottom - L_1) \leq j < bottom$, since the lower bound cannot attain a value less than 1.

The haptic refresh rate is 1 KHz. However the haptic tool is operated by human hand which is very slow as compared to 1000 cycles per second. Effectively most of the haptic samples of velocity end up being zero. In such a case, we enforce the velocity of the previous iteration for the current iteration velocity value, following the principle of inertia of motion.

Even after the redistribution of removed clay volume following equations (5-8), there can be scenarios where the deformation is not volume preserving. This occurs firstly when the clay distribution in the lower cylindrical elements is not complete, that is, $\max(1, bottom - L_1) = 1$. In such a case the algorithm distributes the excess undistributed clay to the upper cylindrical elements following equations (5) and (6).

Secondly when $top + L_1$ is greater than N , then the removed clay is not distributed entirely in the upper cylindrical elements since $\min(top + L_1, N) = N$ in this case. In such cases the excess volume should increase the height of the clay body.

This action is carried out by the following algorithm. Let Δv_{excess} be the amount of undistributed clay, and Δv_N be the normalized volume of the N^{th} cylinder, given by $\Delta v_N = R_N^2 - r_N^2$. To distribute Δv_{excess} amount of clay we employ the following steps.

While($\Delta v_{\text{excess}} > \Delta v_N$) do steps (a) and (b)

(a) Reduce Δv_{excess} by Δv_N amount.

(b) Add a new cylinder above the N^{th} cylinder element and set all its attributes to the N^{th} cylinder's attribute, except for setting its vertical departure from the N^{th} cylinder by h , that is $y_{N+1} = y_N + h$. Increase the number of elements by 1, $N = N + 1$. This renders the effect of placing additional cylinders over the top most cylinder thereby increasing the height of the lump of clay.

The method discussed above for distributing excess clay volume incurs an error in preserving the actual volume, but the error is bounded between $(0, \Delta v_N)$.

6 FORCE FEEDBACK

Whenever the haptic tool touches the clay body, a force is fed back to the haptic device to simulate the feeling of touch. The force feedback is divided into two components. One of which is the spring force caused due to deformation of the clay model. The other component of force is the frictional force which renders a feeling of grip on the rotating clay and is assumed not to deform the object.

6.1 Spring Force

This force is given by Hooke's law and it acts normally at the point of contact of the cylindrical elements with the haptic tool. The total deformation force is given by

$$\vec{F}_d = K \sum_{i=1}^N s_i \vec{f}_i$$

where K is the stiffness constant of the clay, s_i is the collision indicator and \vec{f}_i is the force due the i^{th} cylinder on the haptic tool.

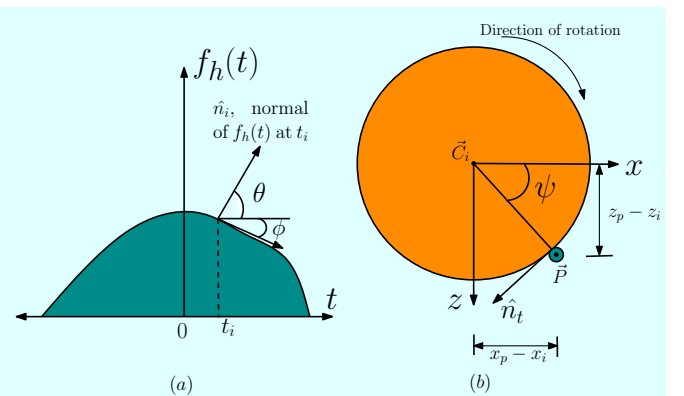


Figure 5: (a) Cross-section of the haptic tool in a plane passing through HIP parallel to y-axis. (b) Cross-section of the i^{th} cylinder in the $x-z$ plane (\hat{n}_t gives the direction of frictional force)

The magnitude of spring force is proportional to the depth of penetration of the haptic tool. For compressive collision, that is $d_i < R_i + f_h(t_i)$, the per element force is given by

$$\vec{f}_i = [d_i - \{R_i + f_h(t_i)\}] \cdot \hat{n}_i$$

Here \hat{n}_i is the normal at the point of contact of the i^{th} cylinder and the haptic tool as shown in figure 5(a).

Similarly for expansive collision, that is $d_i + f_h(t_i) > r_i$, the per element force is given by

$$\vec{f}_i = \{d_i + f_h(t_i) - r_i\} \cdot \hat{n}'_i$$

Where \hat{n}'_i is equal to \hat{n}_i only with its y-component reversed. This is done to render the proper force direction for expansive collision.

The normal \hat{n}_i is a three dimensional unit vector whose direction depends on the shape of the haptic tool and the point of contact of the tool with the clay body in x-z plane. Figure 5(a) gives the cross-section of the haptic tool in a vertical plane. The slope at the point of contact for the i^{th} cylinder is given by the $m_1 = f'_h(t_i)$, where $f'_h(t_i)$ gives the derivative of $f_h(t)$ at $t = t_i$. From the slope the angle ϕ , as shown in figure 5(a), is given by $\phi = \tan^{-1}(m_1)$. The angle θ can be obtained as $\theta = \phi + 90^\circ$. Figure 5(b) reveals the cross section along the x-z plane. The angle ψ can be calculated as $\psi = \tan^{-1}(\frac{z_p - z_i}{x_p - x_i})$.

The unit normal \hat{n}_i vector for compressive collision is given by

$$\hat{n}_i = (\sin \theta \cos \psi, \cos \theta, \sin \theta \sin \psi)$$

The unit normal \hat{n}'_i vector for expansive collision is given by

$$\hat{n}'_i = (\sin \theta \cos \psi, -\cos \theta, \sin \theta \sin \psi)$$

6.2 Frictional Force

During pottery, the clay rotating on the platform offers certain grip to the human hand. This grip is a result of frictional forces at the clay surface. Without frictional force the interaction with the clay model would feel slippery. We model frictional force as a part of the force feedback, directed towards the direction of rotation along the tangential direction at the point of contact. Since frictional force is proportional to the normal force at the point of contact of the tool with the clay body, it is given by

$$\vec{F}_r = \mu |\vec{F}_d| \cdot \hat{n}_i$$

where μ is the co-efficient of dynamic friction of the clay surface, \hat{n}_i is the unit vector at the point of contact along the tangential direction towards the direction of rotation of the clay volume as shown in figure 5.

The total force \vec{F}_{tot} is the summation of the spring force and the frictional force.

$$\vec{F}_{tot} = \vec{F}_d + \vec{F}_r$$

The stiffness constant is chosen in such a way so as to limit the force feedback to 5 N due to limitation of the haptic device.

7 MECHANICAL STABILITY

During real life pottery, conditions may occur when the clay model becomes mechanically unstable. Such conditions may result if the clay model cannot sustain its own weight. In this section, we focus on maintaining the structural stability of the clay body as it is deformed. Since cylinders are stacked up vertically, a cylinder experiences the weight of all the cylinders stacked above it. Therefore every cylinder experiences a stress developed on it as a result of this force. As the external radius R_i and internal radius r_i values come close to each other, stress on the i^{th} element increases. We set a threshold stress that can be tolerated by each cylindrical element. If the stress experienced by an element surpasses the threshold value β_T , then the structure yields to the stress and collapses.

The weight experienced by the i^{th} cylinder M_i is given by,

$$M_i = \sum_{j=i+1}^N m_j$$

where m_j is the mass of the j^{th} cylinder, given as $m_j = \pi h \rho (R_j^2 - r_j^2)$, where ρ gives the constant mass density of the clay.

Now we define stress at the i^{th} cylinder as,

$$\beta_i = \frac{M_i}{\pi(R_i^2 - r_i^2)}$$

If the stress at the i^{th} cylinder exceeds the threshold, $\beta_i > \beta_T$, then the structure collapses down from the i^{th} cylinder onward. The collapse algorithm is a rotation about the center of collapse which is the HIP at the time of collapse.

The reduction in radius, ϵ_{r_i} caused due to deformation, as discussed in section 5, is designed to be proportional to $(R_i - r_i)$ to ensure that the i^{th} cylindrical element does not become very thin, by consequently reducing the value of ϵ_{r_i} . It is not desirable for the difference in the radii for the i^{th} cylinder to take low value because in that case the stress at that cylindrical element will be high and the model is amenable to collapse from the i^{th} cylinder.

8 RESULTS AND CONCLUSIONS

The proposed method has been implemented on a desktop computer running on Windows XP operating system with Intel(R) Core(TM) i7-2600 CPU @ 3.40 GHz, 16GB RAM and NVIDIA GeForce GTX 560i GPU. A 3 degree of freedom Falcon haptic device from NOVINT was used for the haptic interaction. Microsoft Visual C++, 2008 with graphics rendering by OpenGL 2.0 was used for development of the model. Data structure for the attributes of each cylinder was implemented along with the haptic tool. The model starts with a cylindrical stack of rotating mass with no internal deformation ($r_i = 0, \forall i$). Two separate threads for computation of force feedback and clay structure update were used.

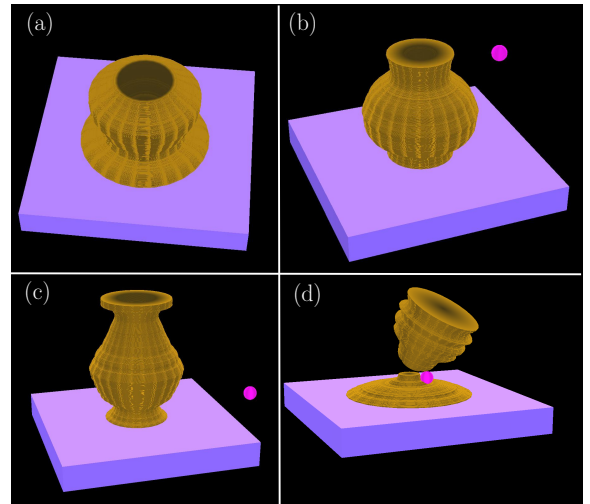


Figure 6: Various pottery models designed by the proposed algorithm. Figure 6(d) illustrates a mechanically unstable pottery structure.

Figure 6 shows various pottery design examples produced by the proposed algorithm using a spherical haptic tool. In each of the

Table 1: Scores given by different users to proposed model in fields of the smoothness of the force and user friendliness

User	Smoothness	User Friendliness	Average
1	7.5	8.5	8
2	8	8.5	8.3
3	8	8	8
4	8	9	8.5
5	7	8	7.5

above finished structures shown in figure 6, the lump of clay consists of 200 cylindrical elements to start with however with increase in height of the clay body, the number of cylindrical elements increased. Figure 6(d) shows the collapse of the lump of clay due to excessive stress on the weakest cylindrical element. The proposed pottery model computes force under 1 ms which is the haptic device rendering speed. The stiffness constant(K) was chosen as 50 units so as to limit the force magnitude to of 5 N.

The performance of this algorithm is of subjective nature and experience may vary between different users. So the following experimental protocol was undertaken. The proposed model was tested by 5 users and scores were given by the user based on their experience. The users were first asked to familiarize themselves with the haptic environment and then they were asked to develop a pottery structure. Users were asked to grade the model out of 10 as regards the smoothness of the force and user friendliness of the model based on their experience. Table 1 shows the scores of 5 users. Based on the scores of the users, the overall merit of the model was calculated as the average of all the scores. The figure of merit for our algorithm from Table 1 is calculated to be 8 out of 10 and the users were satisfied with the end result. However the figure of merit can change for different users based on their experience with the haptic environment.

To investigate the efficiency with which the proposed method preserves volume, we calculated the deviation of the current clay volume from the initial volume. The current clay volume is sum of volume of all the cylindrical elements. Figure 7 shows the variation of error in volume preservation expressed as percentage of initial volume, for the construction of pottery structure shown in figure 6(a). The maximum error in volume preservation for the data shown in figure 7 is found to be 0.44% which is a negligible loss of clay and volume is thus efficiently preserved.

Our algorithm is designed to model volume preserving deformations where the removed clay is redistributed to the other parts of the clay body thereby preserving the total volume. However if the clay is just removed from the surface as a consequence of collision, it would represent a chiseling operation done in actual pottery using a sharp tool where volume is not preserved. Such an application can be implemented if the volume preserving algorithm discussed in section 5.1 is omitted from the overall pottery design algorithm.

In this paper, we have proposed an algorithm for implementing virtual pottery using cylindrical elements. The model assumes that the deformation is circularly symmetric about the axis of rotation of the clay body which provides the key to simple collision detection and response algorithms. The computational model can be rendered in elapsed time of less than 1 ms which is the haptic update rate. We implemented the volume preserving deformation of a rotating clay by redistributing the removed clay from the point of collision. The loss of clay is found to be negligible as compared to initial volume and thus volume is preserved efficiently. We also implemented the mechanical stability aspect by calculating the stress at each cylinder and comparing it with a threshold value.

ACKNOWLEDGEMENTS

Partial financial supports from Bharti Centre for Communication, DST and DEITY are gratefully acknowledged.

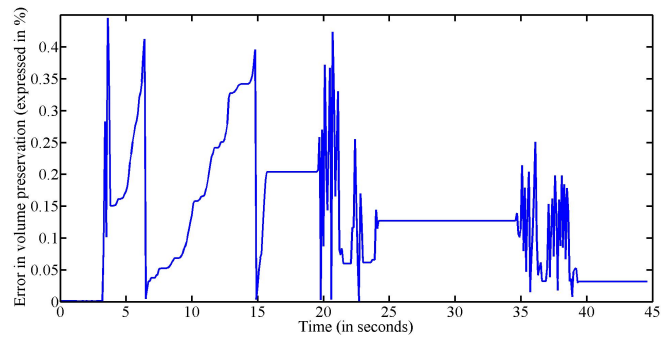


Figure 7: Variation of error in volume expressed as percentage of initial volume for a typical pottery exercise.

REFERENCES

- [1] R. S. Avila and L. M. Sobierajski. A haptic interaction method for volume visualization. In *Visualization '96. Proceedings.*, pages 197–204. IEEE, 1996.
- [2] M.-P. Cani and A. Angelidis. Towards virtual clay. In *ACM SIGGRAPH 2006 Courses, SIGGRAPH '06*, pages 67–83, New York, NY, USA, 2006. ACM.
- [3] I. F. Costa and R. Balaniuk. Lem—an approach for real time physically based soft tissue simulation. In *Robotics and Automation, 2001. Proceedings 2001 ICRA. IEEE International Conference on*, volume 3, pages 2337–2343. IEEE, 2001.
- [4] L. Kim, G. S. Sukhatme, and M. Desbrun. A haptic-rendering technique based on hybrid surface representation. *Computer Graphics and Applications, IEEE*, 24(2):66–75, 2004.
- [5] S. D. Laycock and A. Day. A survey of haptic rendering techniques. In *Computer Graphics Forum*, volume 26, pages 50–65. Wiley Online Library, 2007.
- [6] J. Lee, G. Han, and S. Choi. Haptic pottery modeling using circular sector element method. In *Haptics: Perception, Devices and Scenarios*, pages 668–674. Springer, 2008.
- [7] C. J. Luciano, P. P. Banerjee, and S. H. Rizzi. Gpu-based elastic-object deformation for enhancement of existing haptic applications. In *Automation Science and Engineering, 2007. CASE 2007. IEEE International Conference on*, pages 146–151. IEEE, 2007.
- [8] K. T. McDonnell, H. Qin, and R. A. Wlodarczyk. Virtual clay: A real-time sculpting system with haptic toolkits. In *Proceedings of the 2001 symposium on Interactive 3D graphics*, pages 179–190. ACM, 2001.
- [9] D. C. Ruspini, K. Kolarov, and O. Khatib. The haptic display of complex graphical environments. In *Proceedings of the 24th annual conference on Computer graphics and interactive techniques*, pages 345–352. ACM Press/Addison-Wesley Publishing Co., 1997.
- [10] K. Salisbury, F. Conti, and F. Barbagli. Haptic rendering: introductory concepts. *Computer Graphics and Applications, IEEE*, 24(2):24–32, 2004.
- [11] K. Sreeni and S. Chaudhuri. Haptic rendering of dense 3d point cloud data. In *Haptics Symposium (HAPTICS), 2012 IEEE*, pages 333–339, 2012.
- [12] H. Wang, Y. Wang, and H. Esen. Realization and application of mass-spring model in haptic rendering system for virtual reality. In *Intelligent Computation Technology and Automation, 2009. ICICTA '09. Second International Conference on*, volume 2, pages 156–159. IEEE, 2009.
- [13] C. B. Zilles and J. K. Salisbury. A constraint-based god-object method for haptic display. In *Intelligent Robots and Systems '95. Human Robot Interaction and Cooperative Robots', Proceedings. 1995 IEEE/RSJ International Conference on*, volume 3, pages 146–151. IEEE, 1995.